

## RESEARCH ARTICLE

# The lamin-A/C–LAP2 $\alpha$ –BAF1 protein complex regulates mitotic spindle assembly and positioning

Ran Qi<sup>1,\*</sup>, Nan Xu<sup>1,\*</sup>, Gang Wang<sup>1</sup>, He Ren<sup>1</sup>, Si Li<sup>1</sup>, Jun Lei<sup>1</sup>, Qiaoyu Lin<sup>1</sup>, Lihao Wang<sup>1</sup>, Xin Gu<sup>1</sup>, Hongyin Zhang<sup>2</sup>, Qing Jiang<sup>1,‡</sup> and Chuanmao Zhang<sup>1,‡</sup>

**ABSTRACT**

Some nuclear proteins that are crucial in interphase relocate during the G2/M-phase transition in order to perform their mitotic functions. However, how they perform these functions and the underlying mechanisms remain largely unknown. Here, we report that a fraction of the nuclear periphery proteins lamin-A/C, LAP2 $\alpha$  and BAF1 (also known as BANF1) relocate to the spindle and the cell cortex in mitosis. Knockdown of these proteins by using RNA interference (RNAi) induces short and fluffy spindle formation, and disconnection of the spindle from the cell cortex. Disrupting the microtubule assembly leads to accumulation of these proteins in the cell cortex, whereas depolymerizing the actin microfilaments results in the formation of short spindles. We further demonstrate that these proteins are part of a stable complex that links the mitotic spindle to the cell cortex and the spindle matrix by binding to spindle-associated dynein, the actin filaments in the cell cortex and the spindle matrix. Taken together, our findings unveil a unique mechanism where the nuclear periphery proteins lamin-A/C, LAP2 $\alpha$  and BAF1 are assembled into a protein complex during mitosis in order to regulate assembly and positioning of the mitotic spindle.

**KEY WORDS:** BAF1, LAP2, Cell cycle, Lamin-A/C, Spindle assembly, Spindle positioning

**INTRODUCTION**

Mitotic spindle assembly and positioning are dynamic processes in mammalian cells that require precise coordination of nuclear disassembly, chromatin condensation, microtubule cytoskeleton reorganization and microtubule–kinetochore connections during entry into mitosis (Grill and Hyman, 2005; Kiyomitsu and Cheeseman, 2012; Lancaster and Baum, 2011; Scholey et al., 2003; Verlhac, 2011; Walczak and Heald, 2008). During these processes, some nuclear proteins relocate to the spindle in order to perform distinct roles (Fu et al., 2010; Galli et al., 2011; Luxenburg et al., 2011; Markus and Lee, 2011; Orjalo et al., 2006; Tsai et al., 2006; Weber et al., 2004; Wühr et al., 2008; Yi et al., 2011), although the mechanisms are largely unclear.

Lamins, LAP2 $\alpha$  (encoded by a splice variant of the *TMPO* mRNA) and barrier-to-autointegration factor 1 (BAF1; also known as BANF1) are components of the nuclear periphery in interphase and play crucial roles in the nucleus, such as nuclear structure

maintenance, DNA replication and regulation of gene transcription (Hutchison, 2002; Mekhail and Moazed, 2010). Lamins can be classified as type A and type B and are the main components of the nuclear lamina. A-type lamins, including lamin-A and lamin-C (both encoded by *LMNA*; herein referred to as Lamin-A/C) are found mainly in differentiated tissues, whereas B-type lamins (lamin-B, encoded by *LMNB1*) are required for cell survival (Burke and Stewart, 2013; Hutchison, 2002). LAP2 $\alpha$  is a member of the lamina-associated-polypeptide-2-family proteins, which are tightly associated with the nuclear lamina (Burke and Stewart, 2002). LAP2 $\alpha$  forms a stable complex with lamin-A/C in the nucleoplasm in interphase cells in order to maintain the cell in a proliferative state by controlling localization and phosphorylation of the retinoblastoma-associated protein (Rb) (Dechat et al., 2000; Pekovic et al., 2007). LAP2 $\alpha$  can also regulate the nucleoplasmic lamin-A/C pool, but the mechanisms remains elusive (Gesson et al., 2014). BAF1 is an evolutionarily conserved small protein that binds to chromatin DNA and histones. It also binds to LAP2, emerin and MAN1 (LEM) proteins on the inner nuclear membrane and connects the nuclear envelope to chromatin. BAF1 might also form a link between the nuclear envelope, the nuclear lamina and chromatin (Güttinger et al., 2009). The function of BAF1 is so far not very clear. It has been found to be required for chromosome segregation and nuclear envelope assembly (Margalit et al., 2005). BAF1 might also be an essential protein because RNAi-mediated knockdown of BAF1 is lethal in *Caenorhabditis elegans* (Zheng et al., 2000).

Mutations of lamin-A/C cause a variety of diseases called laminopathies or nuclear envelopopathies (Burke and Stewart, 2006; Gruenbaum et al., 2005; Verstraeten et al., 2007), whereas a mutation in BAF1 has been associated with a progeroid syndrome (Puente et al., 2011). Although these proteins are nuclear in interphase, and their roles have been extensively studied, how they perform their distinct roles in mitosis at the molecular level remains elusive. It is also unclear whether the related diseases are caused by dysfunction of these proteins in interphase or mitosis during the cell cycle. In this work, we report that lamin-A/C, LAP2 $\alpha$  and BAF1 are assembled into a stable complex in mitosis that regulates mitotic spindle assembly and positioning.

**RESULTS**

## Microtubule- and microfilament-dependent localization of lamin-A/C, LAP2 $\alpha$ and BAF1 to the mitotic spindle and the cell cortex

To investigate the mitotic roles of the nuclear periphery proteins during the cell cycle, we studied the dynamic localizations of lamin-A/C, LAP2 $\alpha$  and BAF1 proteins that had been tagged with green fluorescent protein (GFP) or other tags in HeLa cells. Under a fluorescence microscope, we first observed that a fraction of lamin-A/C, LAP2 $\alpha$  and BAF1 relocated to the cell cortex and the spindle

<sup>1</sup>The Ministry of Education Key Laboratory of Cell Proliferation and Differentiation and the State Key Laboratory of Membrane Biology, College of Life Sciences, Beijing 100871, China. <sup>2</sup>Cancer Research Center, Peking University Hospital, Peking University, Beijing 100871, China.

\*These authors contributed equally to this work

‡Authors for correspondence (jiangqing@pku.edu.cn; zhangcm@pku.edu.cn)

Received 13 October 2014; Accepted 15 June 2015

in mitosis, although some LAP2 $\alpha$  and BAF1 associated with the chromosomes (Fig. 1A; supplementary material Fig. S1A). By using immunofluorescent labeling, the endogenous lamin-A/C, LAP2 $\alpha$  and BAF1, as well as Myc-tagged lamin-A, were also observed on the spindle and the cell cortex (Fig. 1B; supplementary material Fig. S1B). When the cells were treated with nocodazole to depolymerize microtubules, a proper mitotic spindle could not be assembled and, because there was no spindle to which these proteins could relocate, a large portion of these proteins only localized at the cell cortex (Fig. 1C; supplementary material Fig. S1C), indicating that these proteins were linked with the microtubules of both spindle and spindle-pole asters. When the cells were treated with either cytochalasin D to depolymerize the microfilaments or latrunculin A to inhibit G-actin from polymerizing into the actin microfilaments, the localization of lamin-A/C, LAP2 $\alpha$  and BAF1 to the cell cortex

and spindle was obviously disturbed (Fig. 1C), suggesting that depolymerization of actin filaments causes withdrawal of these proteins from the cell cortex and the spindle. The cells were also treated with the myosin-II inhibitor Y-27632, which interrupts the binding of myosin II to actin (Rosenblatt et al., 2004), and the results showed that the localization of lamin-A/C, LAP2 $\alpha$  and BAF1 to the cell cortex was abolished, and localization to the spindle was also largely reduced (Fig. 1D; supplementary material Fig. S1D–G), suggesting that disrupting the connection of myosin II with actin filaments also induces withdrawal of these proteins from the cell cortex and the basic structures of the spindle. Taken together, these data indicate that a fraction of the lamin-A/C, LAP2 $\alpha$  and BAF1 pool localizes to the cell cortex and the spindle in a manner that is dependent on the cross-interaction of actin filaments and microtubules.

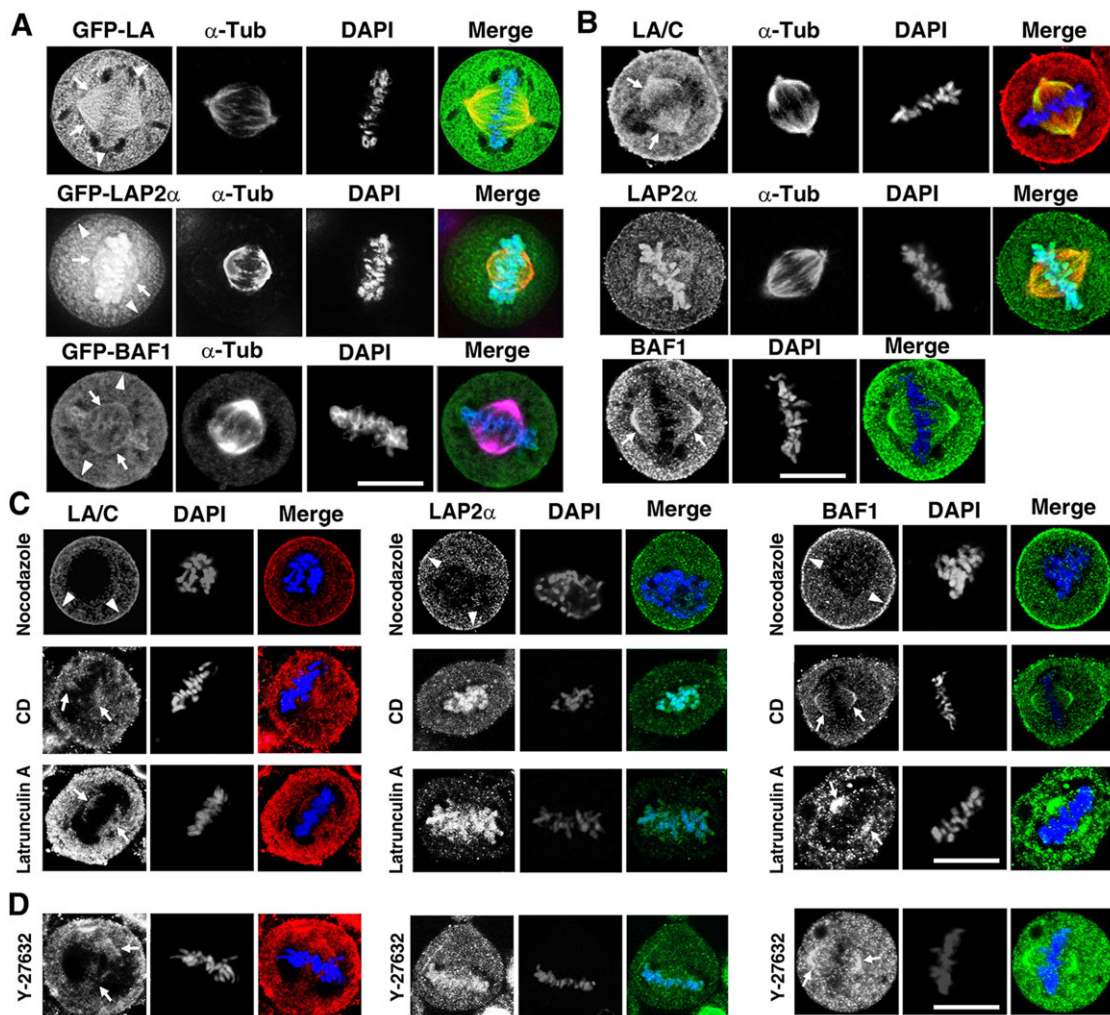


**Fig. 1. Lamin-A/C, LAP2 $\alpha$  and BAF1 localize to the mitotic spindle and cell cortex in a microtubule- and microfilament-dependent manner.** (A) HeLa cells that transiently expressed GFP-tagged lamin-A (LA), LAP2 $\alpha$  or BAF1 were fixed and immunostained with an antibody against  $\alpha$ -tubulin. DNA was stained with DAPI. Note that exogenous GFP-lamin-A, GFP-LAP2 $\alpha$  and GFP-BAF1 localize to both the mitotic spindle (arrows) and the cell cortex (arrowheads). (B) Endogenous lamin-A/C (LA/C), LAP2 $\alpha$ , BAF1 and  $\alpha$ -tubulin were immunostained using specific antibodies. DNA was labeled with DAPI. Note the spindle (arrows) and cell cortex (arrowheads) staining of lamin-A/C, LAP2 $\alpha$  and BAF1. (C) HeLa cells were treated with nocodazole to depolymerize microtubules, or with cytochalasin D (CD) or latrunculin A to depolymerize actin filaments, followed by immunostaining for endogenous lamin-A/C, LAP2 $\alpha$  and BAF1. DNA was labeled with DAPI. Note that treatment with nocodazole largely reduced the localization at the spindle but not at the cell cortex (arrowheads) of lamin-A/C, LAP2 $\alpha$  and BAF1, whereas treatment with cytochalasin D and latrunculin A almost abolished the localization at the cell cortex (arrowheads) and substantially reduced the localization at the spindle (arrows) of these proteins. (D) HeLa cells were treated with the myosin-II inhibitor Y-27632 to inhibit the interaction of actin with myosin and were then immunostained for lamin-A/C, LAP2 $\alpha$  and BAF1. DNA was labeled with DAPI. Note that this treatment abolished the localization at the cell cortex and reduced the localization at the spindle (arrows) of lamin-A/C, LAP2 $\alpha$  and BAF1. Scale bars: 10  $\mu$ m.

## Lamin-A/C, LAP2 $\alpha$ and BAF1 are required for proper spindle assembly

To determine the functions of lamin-A/C, LAP2 $\alpha$  and BAF1 at the spindle and the cell cortex, we knocked down these proteins by using RNAi and found that a reduction in the amount of these

proteins resulted in abnormal spindle assembly, as measured and quantified in three assays (Fig. 2A,B; supplementary material Fig. S2A). First, the percentage of multi-polar spindles was increased (Fig. 2C); second, the number of the short spindles (pole-to-pole spindle length  $<8\ \mu\text{m}$ ) was significantly increased

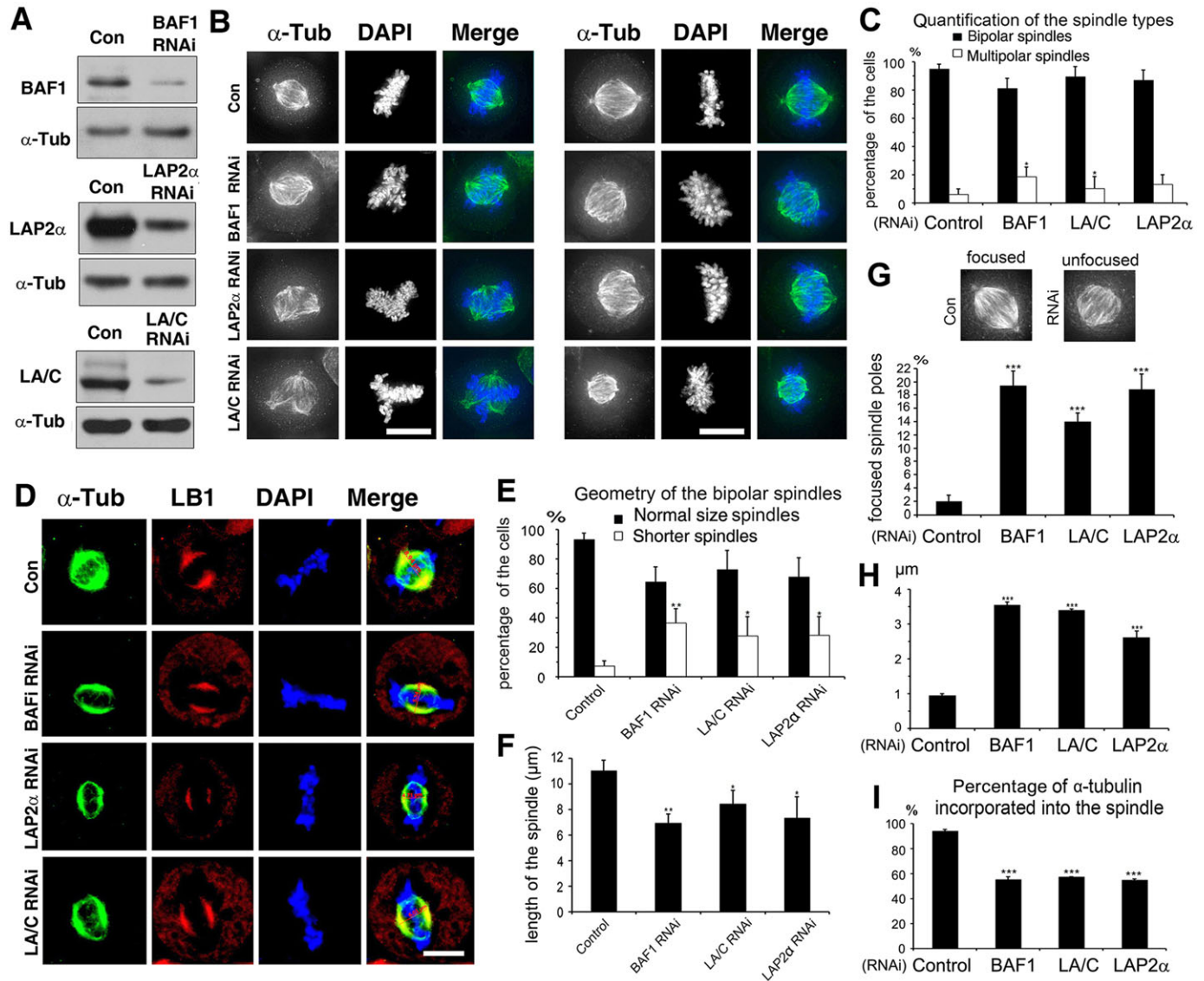


**Fig. 2. Knockdown of lamin-A/C, LAP2 $\alpha$  and BAF1 affects proper spindle assembly and results in short spindle formation.** (A) RNAi knockdown of lamin-A/C (LA/C), LAP2 $\alpha$  and BAF1 in HeLa cells.  $\alpha$ -Tubulin ( $\alpha$ -Tub) was probed as a loading control. (B) Cells with knockdown of lamin-A/C, LAP2 $\alpha$  or BAF1 were immunostained with an antibody against  $\alpha$ -tubulin in order to visualize the spindles. DNA was labeled with DAPI. The left panel shows the cells with multipolar spindles and the right panels show those with abnormal bipolar spindles in the protein-knockdown cells. Note that both the abnormal bipolar and multipolar spindles are shorter than those in the control (Con) cells. (C) Statistical analyses of abnormal bipolar and multipolar spindles in lamin-A/C-, LAP2 $\alpha$ - or BAF1-knockdown cells. In control cells, 95% of spindles were normal (bipolar) and only 5% were abnormal (multipolar). Three independent experiments were performed, and 100 mitotic cells were counted in each sample;  $*P<0.05$ , by ANOVA. (D) Cells with lamin-A/C-, LAP2 $\alpha$ - or BAF1-knockdown were immunostained. Note that the lamin-B spindle matrix (red) was obviously reduced and smaller than the spindle (green). (E) Percentage of cells with abnormal bipolar spindles in lamin-A/C-, LAP2 $\alpha$ - or BAF1-knockdown cells. A short spindle has been defined as less than  $8\ \mu\text{m}$  in length and a normal spindle as over  $8\ \mu\text{m}$  in length. Three independent experiments were performed, and 300 mitotic cells were counted in each sample;  $*P<0.05$ ,  $**P<0.01$ . (F) Pole-to-pole spindle length analysis. Three independent experiments were performed, and 200 mitotic cells were counted in each sample;  $*P<0.05$ ,  $**P<0.01$ . Note that the average spindle length in control cells was about  $11\ \mu\text{m}$ , whereas in lamin-A/C-, LAP2 $\alpha$ - or BAF1-knockdown cells the spindle length was reduced to less than  $8\ \mu\text{m}$ . (G) Statistical analysis of unfocused abnormal bipolar spindles. The upper panel shows examples of the focused and unfocused spindles. The bottom panel shows the statistical results from three independent RNAi knockdown experiments, and 300 mitotic cells were counted in each sample;  $***P<0.001$ . (H) Statistical analysis of the difference in the distance of the two spindle poles from the nearest point at the cell cortex. The distance of the two spindle poles from the nearest point at the cell cortex was measured by using ImageJ software. Note that in the knockdown cells, the difference in the distance was significantly increased, compared with the control. (I) Analysis of the total amount of  $\alpha$ -tubulin protein in the spindle. The intensity of the fluorescence of  $\alpha$ -tubulin staining was measured by using ImageJ software. Three independent experiments were performed, and 50 mitotic cells were counted in each sample,  $***P<0.001$ . Data are means $\pm$ s.d. Scale bars:  $10\ \mu\text{m}$ .

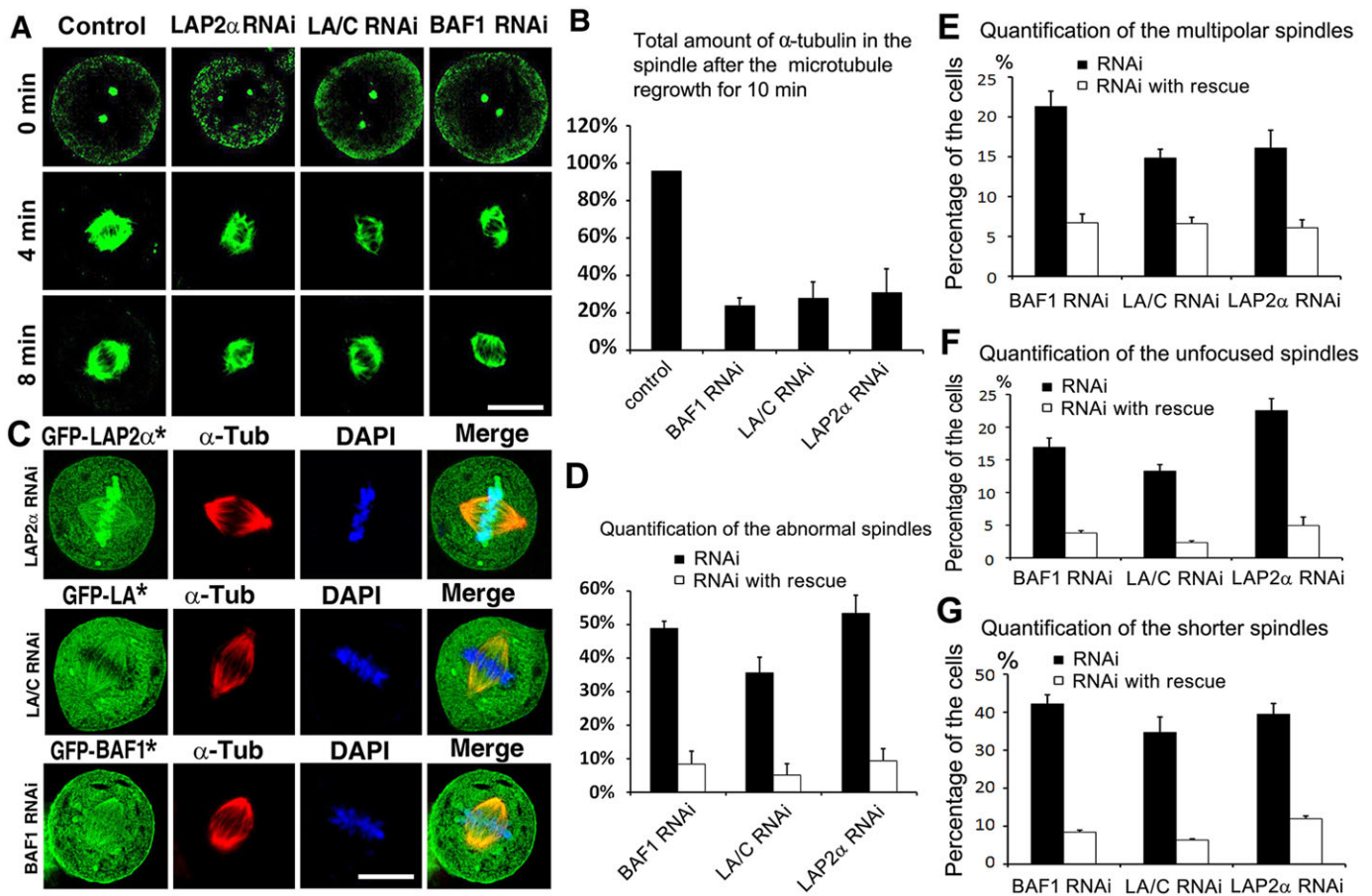


**Fig. 3. Lamin-A/C, LAP2 $\alpha$  and BAF1 knockdown impairs microtubule regrowth.** (A) Microtubule regrowth assay. Note that the microtubule regrowth was obviously impaired in lamin-A/C (LA/C)-, LAP2 $\alpha$ - and BAF1-knockdown cells. (B) Measurement of the relative intensity of microtubules in the spindle 10 min after release from cold temperatures in the control and lamin-A/C-, LAP2 $\alpha$ - or BAF1-knockdown cells. The intensity of the fluorescence of microtubules was measured using ImageJ, and three independent experiments were performed. (C) Rescue of the spindle assembly defects in lamin-A/C-, LAP2 $\alpha$ - and BAF1-knockdown cells by expressing RNAi-resistant lamin-A, LAP2 $\alpha$  or BAF1 (asterisks). Note that the exogenous protein expression rescued the spindle assembly defects caused by lamin-A/C-, LAP2 $\alpha$ - or BAF1-knockdown in HeLa cells. (D) Quantification of the percentages of the metaphase cells with abnormal spindles. Three independent experiments were performed, and more than 150 metaphase cells in each group were analyzed. (E) Quantification of the percentages of the cells with multipolar spindles in lamin-A/C-, LAP2 $\alpha$ - and BAF1-RNAi knockdown and the equivalent rescue cells. Note that the exogenous protein expression rescued the multipolar spindle defects caused by lamin-A/C-, LAP2 $\alpha$ - or BAF1-knockdown in HeLa cells. Three independent experiments were performed, and 100 mitotic cells were counted in each sample. (F) Quantification of the cells with unfocused spindles in lamin-A/C-, LAP2 $\alpha$ - and BAF1-knockdown cells and the equivalent rescue cells. Note that exogenous protein expression rescued the unfocused spindle defects caused by lamin-A/C-, LAP2 $\alpha$ - or BAF1-knockdown in HeLa cells. Three independent experiments were performed, and 100 mitotic cells were counted in each sample. (G) Quantification of the cells with shorter spindles (a spindle length less than 8  $\mu$ m) in lamin-A/C-, LAP2 $\alpha$ - or BAF1-knockdown cells and the equivalent rescue cells. Note that the exogenous protein expression rescued the shorter spindle defects caused by lamin-A/C-, LAP2 $\alpha$ - or BAF1-knockdown in HeLa cells. Three independent experiments were performed, and 100 mitotic cells were counted in each sample. Data are means $\pm$ s.d. Scale bars: 10  $\mu$ m.

(Fig. 2E); and third, the spindles were obviously not centered in the cell (Fig. 2D). Cells that had been subjected to triple RNAi against lamin-A/C, LAP2 $\alpha$  and BAF1 were subsequently stained with an antibody against lamin-B. Quantification by using microscopy demonstrated that, although the treatment did not change the total protein level of lamin-B (supplementary material Fig. S2B), the lamin-B spindle matrix was obviously reduced (Fig. 2D). This result supports the hypothesis that these proteins are involved in regulating the spindle matrix assembly. We also found that knocking down any of the proteins lamin-A/C, LAP2 $\alpha$  or BAF1 reduced the localization of the other two proteins to the spindle and cell cortex (supplementary material Fig. S2B), indicating that the three proteins work in a synergistic manner. Furthermore, the spindle poles in lamin-A/C-, LAP2 $\alpha$ - and BAF1-knockdown cells were significantly unfocused, and the spindles had swelled (Fig. 2B,D,G). Remarkably, the length of the spindles was

reduced by 25–33% (Fig. 2F). In most of the knockdown cells, the difference in the distance of the two spindle poles from the nearest point at the cell cortex was also significantly increased (Fig. 2H). Moreover, the amount of  $\alpha$ -tubulin that had been incorporated into the spindle microtubules in the knockdown cells was also reduced, as quantified by measuring by the fluorescence intensity with ImageJ software (Fig. 2I), suggesting that microtubule formation had been compromised.

To understand whether lamin-A/C, LAP2 $\alpha$  and BAF1 are required for mitotic spindle assembly, we subjected cells that expressed GFP-tubulin to cold temperatures, which disassembles microtubules, and examined the ability of the mitotic spindle microtubules to regrow after release at a warmer temperature. By using live-imaging microscopy, we observed that, in control metaphase cells, the microtubules re-grew to form a full-size spindle within 10 min of release, whereas in lamin-A/C-, LAP2 $\alpha$ - or

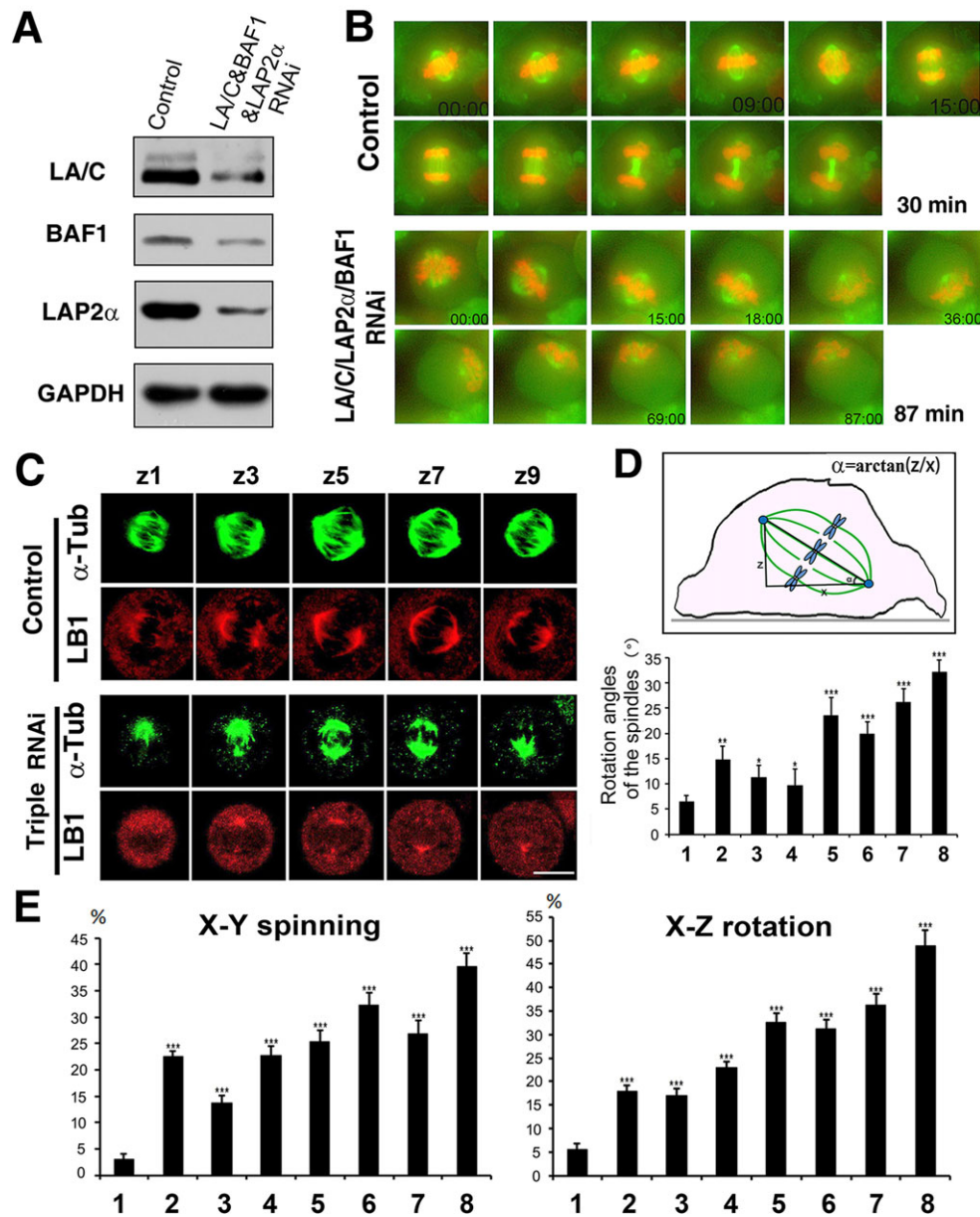


**Fig. 4. Lamin-A/C, LAP2 $\alpha$  and BAF1 regulate mitotic spindle positioning and orientation.** (A) The efficiency of RNAi-mediated triple-knockdown of lamin-A/C, LAP2 $\alpha$  and BAF1 (LA/C&BAF1&LAP2 $\alpha$  RNAi) in HeLa cells that stably expressed GFP- $\alpha$ -tubulin. The cells were transfected with siRNAs against lamin-A/C, LAP2 $\alpha$  and BAF1 simultaneously. Total protein lysates were immunoblotted with the antibodies against lamin-A/C (LA/C), LAP2 $\alpha$  and BAF1. GAPDH was probed using a specific antibody as a loading control. (B) Time-lapse observations of the control and lamin-A/C, LAP2 $\alpha$  and BAF1 triple-knockdown cells that stably expressed GFP- $\alpha$  tubulin (green) and transiently expressed red fluorescent protein (RFP)-tagged histone 2B (red). Images were captured every 3 min. Note that the time from metaphase to the end of telophase in control cells lasted about 30 min, and that the spindle positioning and orientation were clearly normal. By contrast, in lamin-A/C, LAP2 $\alpha$  and BAF1 triple-knockdown cells, the spindle randomly and rapidly roamed, and the metaphase–anaphase transition did not occur. (C) Lamin-A/C, LAP2 $\alpha$  and BAF1 triple-knockdown (triple RNAi) caused mitotic spindle rotation.  $\alpha$ -Tubulin ( $\alpha$ -Tub) and lamin-B1 (LB1) were immunostained with specific antibodies. Different layers of the mitotic spindle along the z-axis (z1–z9 represent images taken through the z-axis) in control and in lamin-A/C, LAP2 $\alpha$  and BAF1 triple-knockdown cells are shown. Note that the two spindle poles of the control cell localized in the same layer parallel with the coverslip surface; whereas in lamin-A/C, LAP2 $\alpha$  and BAF1 triple-knockdown cells, one of the two spindle poles moved up and down along the z-axis. Scale bar: 10  $\mu$ m. (D, upper panel) Schematic showing the calculation of the elevation angle  $\alpha = \arctan(z/x)$ . (Lower panel) The elevation angles for cells shown in C with statistical analysis of the elevation angle  $\alpha$  in x–z axes of the two spindle poles. Three independent experiments were performed,  $n=100$  cells per group; \* $P<0.05$ , \*\* $P<0.01$ , \*\*\* $P<0.001$ . (E) Percentage of cells in which the spindle position deviated in the x–y–z axes in the control cells and the single-, double- or triple-knockdown of lamin-A/C, LAP2 $\alpha$  and BAF1. The live cells shown in B with distinct spindle positions were counted. The left panel shows spindle spinning in the x–y axes, whereas the right panel shows the spindle rotation in the x–z axes. Three independent experiments were performed,  $n=200$  mitotic cells per group; \*\*\* $P<0.001$ . Columns 1–8 in D and E stand for control RNAi, BAF1 RNAi, lamin-A/C RNAi, LAP2 $\alpha$  RNAi, BAF1 and lamin-A/C double RNAi, lamin-A/C and LAP2 $\alpha$  double RNAi, BAF1 and LAP2 $\alpha$  double RNAi, and lamin-A/C triple RNAi, respectively. Note that more than forty of the spindles in triple-knockdown cells were abnormally positioned. Data are means $\pm$ s.d.

BAF1-knockdown cells, the spindle did not regrow normally to form the correct shape, and the intensity of the fluorescence of the spindle was significantly lower (Fig. 3A,B), indicating that the

ability of the microtubules to regrow in lamin-A/C-, LAP2 $\alpha$ - and BAF1-knockdown cells was obviously impaired. Next, we tried to rescue the spindle assembly defects by expressing GFP-fused

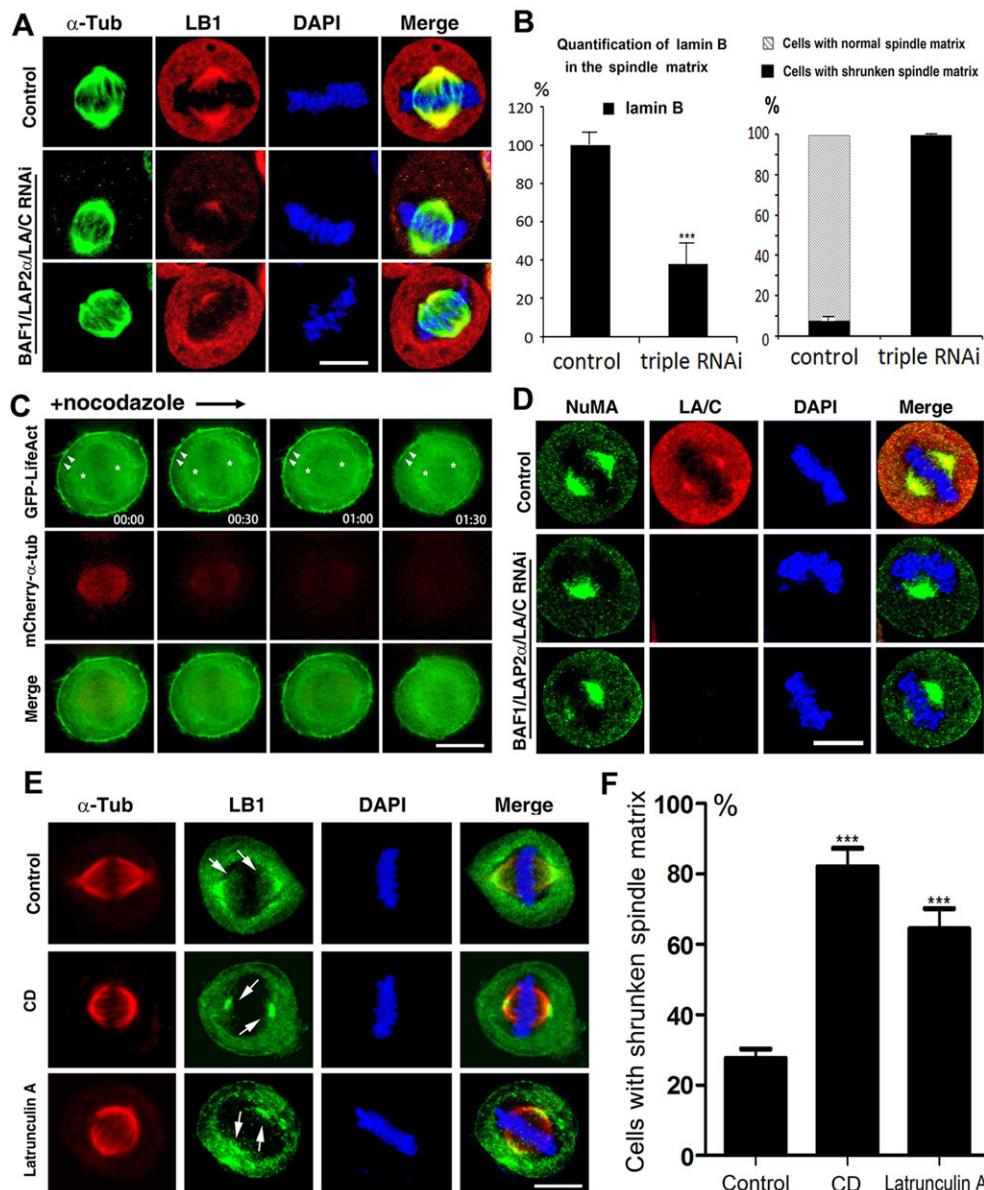


**Fig. 5. Lamin-A/C, LAP2 $\alpha$  and BAF1 target the spindle to the spindle matrix by regulating the spindle matrix assembly.** (A) The spindle matrix in the control and lamin-A/C (LA/C), LAP2 $\alpha$  and BAF1 triple-knockdown cells. The cells were immunostained for  $\alpha$ -tubulin ( $\alpha$ -Tub) and lamin-B1 (LB1) with specific antibodies. DNA was labeled with DAPI. Note that the lamin-B1 spindle matrix was much smaller than the spindle in lamin-A/C, LAP2 $\alpha$  and BAF1 triple-knockdown cells. (B) Measurements of the relative amounts of lamin-B1 in the spindle matrix in control and lamin-A/C, LAP2 $\alpha$  and BAF1 triple-knockdown cells by using ImageJ (left panel), and the spindle matrix size is given in the right-hand panel. Three independent experiments were performed;  $n=100$  cells per group,  $***P<0.001$ . (C) HeLa cells grown in glass-bottomed dishes were co-transfected with GFP-LifeAct and mCherry- $\alpha$ -tubulin (mCherry- $\alpha$ -tub) vectors for 24 h and processed for time-lapse microscopy. Note that GFP-LifeAct (green) labeled the spindle matrix (\*) and the cell cortex (arrowheads), whereas mCherry- $\alpha$ -tubulin was incorporated into the mitotic spindle (red). When the cell was treated with nocodazole at a concentration of 1  $\mu$ g/ml, the spindle microtubules were rapidly depolymerized, whereas the spindle matrix with GFP-LifeAct remained. The time (min) after treatment with nocodazole is given. (D) Lamin-A/C, LAP2 $\alpha$  and BAF1 triple-knockdown does not interfere with mitotic spindle localization of SAFs. HeLa cells were transfected with siRNAs to knock down BAF1, LAP2 $\alpha$ , and lamin-A/C, followed by immunostaining with an antibody against NuMA. The knockdown efficiency was checked by staining of lamin-A/C with a specific antibody. Note that NuMA still localized on the spindle in Lamin-A/C, LAP2 $\alpha$  and BAF1 triple-knockdown cells, although the localization might not be symmetrical compared with that of control. DNA was labeled with DAPI. (E) HeLa cells grown in glass-bottomed dishes were treated with cytochalasin D (CD) for 30 min to depolymerize the actin filaments, or latrunculin A for 30 min to inhibit the microfilament polymerization, and DMSO was used as a control. The cells were immunostained with an antibody against lamin-B1 for the lamin-B spindle matrix (arrows) and an antibody against  $\alpha$ -tubulin ( $\alpha$ -Tub) for the spindle. DNA was labeled with DAPI. Note that treatment with cytochalasin D or latrunculin A substantially induced the lamin-B spindle matrix shrinkage (lamin-B spindle matrix size to  $\alpha$ -tubulin spindle size ratio  $<70\%$ ). (F) Statistical analysis of the lamin-B1 spindle matrix in the control (DMSO) and cytochalasin-D- or latrunculin-A-treated cells with ImageJ. Three independent experiments were performed,  $n=100$  cells per group;  $***P<0.001$ . Data are means $\pm$ s.d. Scale bars: 10  $\mu$ m.

lamin-A, LAP2 $\alpha$  and BAF1 to see whether the defects were due to the knockdown of specific proteins. The results showed that expression of these proteins greatly rescued the defects caused by knockdown of lamin-A/C, LAP2 $\alpha$  and BAF1 (Fig. 3C–G). From

these results, it can be concluded that the spindle localization of lamin-A/C, LAP2 $\alpha$  and BAF1 is required in order to regulate spindle microtubule dynamics and formation of the lamin-B spindle, ensuring proper spindle assembly.

### Lamin-A/C, LAP2 $\alpha$ and BAF1 regulate mitotic spindle positioning and orientation

Given that lamin-A, LAP2 $\alpha$  and BAF1 knockdown can result in aberrant spindle formation in cells (Fig. 2E), we knocked down these proteins in HeLa cells that stably expressed GFP- $\alpha$ -tubulin in order to follow the spindle dynamics with time-lapse microscopy (Fig. 4A,B). Surprisingly, we found that the metaphase–anaphase transition did not occur in cells in which lamin-A, LAP2 $\alpha$  and BAF1 had been simultaneously knocked down (Fig. 4B;

supplementary material Fig. S3A–D). The mitotic spindles were short, collapsed, and moved and rotated randomly in  $x$ ,  $y$  and  $z$  axes in the cells, suggesting that the structure was not only severely affected by knockdown of these proteins, but also the positioning and orientation of the spindles. The cells were subsequently fixed, and the rotation angles of the spindles relative to the horizontal plane were measured (Fig. 4C,D; supplementary material Fig. S4). In most of the knockdown cells, the angle [ $\alpha = \arctan(z/x)$ ] of the spindles in the  $x$ – $z$  axis ranged from over  $10^\circ$  in single-protein-

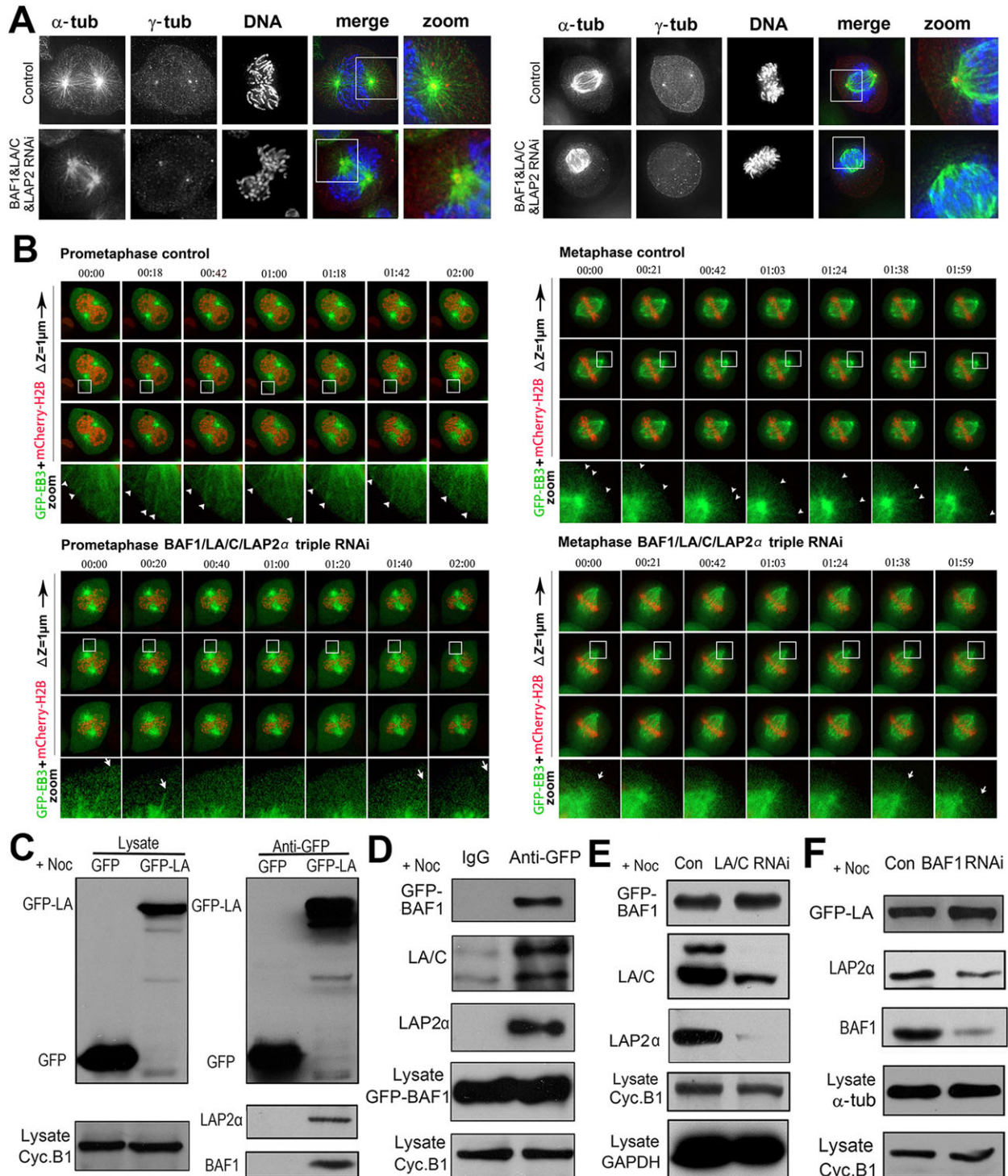


Fig. 6. See next page for legend.

**Fig. 6. Lamin-A/C, LAP2 $\alpha$  and BAF1 form a stable protein complex that links the spindle with the spindle matrix and the cell cortex.** (A) Cells were co-transfected with siRNAs for simultaneous knockdown of lamin-A/C, LAP2 $\alpha$  and BAF1 (BAF1&LA/C&LAP2 RNAi), and immunostained for  $\alpha$ - and  $\gamma$ -tubulin ( $\alpha$ -tub and  $\gamma$ -tub, respectively) using antibodies specific for the proteins. DNA was labeled with DAPI. The left and right panels showed prometaphase and metaphase cells, respectively. Note that the astral microtubule length was much shorter in lamin-A/C, LAP2 $\alpha$  and BAF1 triple-knockdown cells than in control cells. Most of these astral microtubules in the triple-knockdown cells could not reach the cell cortex. (B) Endogenous lamin-A/C, LAP2 $\alpha$ , BAF1 were knocked down simultaneously in HeLa cells. Expression of red fluorescent protein (RFP)-tagged histone 2B was used as a transfection and chromatin indicator. A construct encoding GFP–EB3, which binds to the positive-end of microtubules, was transfected 24 h after the siRNA transfection, and images in different layers along the z-axis of five cells were taken. Boxed areas correspond to the zoom images. Note that the astral microtubules could not effectively link to the cell cortex in lamin-A/C, LAP2 $\alpha$ , BAF1 triple-knockdown prometaphase and metaphase cells, although they were dynamic (arrows), and in the control prometaphase and metaphase cells, the astral microtubules could effectively link to the cell cortex (arrowheads, also see the related full montages in supplementary material Fig. S4). Images were taken at the indicated times (minutes:seconds), time zero represents the beginning of image capture. (C–F) Lamin-A/C, LAP2 $\alpha$  and BAF1 are in a complex in mitosis. HeLa cells stably expressing GFP–lamin-A (GFP–LA; panel C) and GFP–BAF1 (D) were synchronized into prometaphase by using nocodazole (+ Noc), and the GFP proteins were immunoprecipitated with an antibody against GFP. The co-immunoprecipitated proteins were probed with antibodies against BAF1 and LAP2 $\alpha$  by western blotting. Cyclin B1 in the total lysate (Lysate Cyc.B1) was labeled as mitosis indicator and protein loading control. (E) Lamin-A/C was knocked down in HeLa cells that stably expressed GFP–BAF1. The cells were synchronized in prometaphase by using nocodazole. The GFP–BAF1 proteins were immunoprecipitated and the co-immunoprecipitated proteins were probed with antibodies as indicated. Lysate cyclin B1 and GAPDH were probed as a mitosis indicator and protein loading control, respectively. (F) BAF1 was knocked down in HeLa cells that stably expressed GFP–lamin-A (GFP–LA), and the cells were synchronized in prometaphase by using nocodazole. GFP–lamin-A was immunoprecipitated with an antibody against GFP, and the co-immunoprecipitated proteins were probed with the antibodies against LAP2 $\alpha$  and BAF1.  $\alpha$ -Tubulin and cyclin B1 were probed in the total lysates as a protein loading control and mitosis indicator, respectively. Con, control; LA/C, lamin-A/C.

knockdown cells up to 42° in triple-protein-knockdown cells, whereas in the control cells the angle was not more than 7° (Fig. 4D). We also observed that the percentage of the cells with a deviation in spindle positioning was significantly increased in all single-protein-knockdown cells, and especially so in double- and triple-knockdown cells (Fig. 4D,E). These results indicate that knockdown of lamin-A/C, LAP2 $\alpha$  and BAF1 interrupts the connection of the spindle with the cell cortex, resulting in the spindle positioning and orientation failure, and the spindle roaming.

We also studied the relationship between the spindle microtubules and the spindle matrix (Yao et al., 2012; Zheng, 2010) in lamin-A, LAP2 $\alpha$  and BAF1 triple-knockdown cells. We observed that the spindle matrix was not only small and morphologically abnormal, but also that the spindle was obviously swollen and separated from the lamin-B spindle matrix in the knockdown cells due to the spindle matrix shrinkage (Fig. 5A,B). Because it has been reported that some F-actin is organized into a spindle-like F-actin structure in late meiosis I of mouse oocytes (Azoury et al., 2008), to confirm the localization of F-actin at the spindle area, we co-expressed GFP–LifeAct, which specifically labels F-actin and mCherry– $\alpha$ -tubulin, in order to label microtubules. By using time-lapse microscopy, we confirmed that the actin filaments were at both the spindle area and the cell cortex. When metaphase cells were treated with nocodazole to depolymerize the spindle microtubules, we observed that

GFP–LifeAct still remained on the basic spindle structure, the spindle matrix (Fig. 5C). We also immunostained one of the spindle assembly factors (SAFs), NuMA (also known as NuMA1), and found that the spindle localization of NuMA was not affected in lamin-A/C, LAP2 $\alpha$  and BAF1 triple-knockdown cells (Fig. 5D), indicating that knocking down lamin-A/C, LAP2 $\alpha$  and BAF1 does not prevent the SAFs from localizing to the spindle for spindle assembly. Then, we treated the cells with cytochalasin D and latrunculin A to depolymerize the actin filaments, and we immunostained  $\alpha$ -tubulin and lamin-B1 in order to observe the spindle and the spindle matrix, respectively. We found that the spindle matrix had significantly shrunk in cytochalasin-D- or latrunculin-A-treated cells (Fig. 5E,F). Taken together, these data indicate that lamin-A/C, LAP2 $\alpha$  and BAF1 also connect the spindle with the cell cortex and anchor the spindle to the spindle matrix by connecting with the spindle-matrix-based actin filaments.

### Lamin-A/C, LAP2 $\alpha$ and BAF1 are assembled into a stable protein complex that links the spindle with the spindle matrix and the cell cortex

Next, we decided to investigate how the lamin-A/C, LAP2 $\alpha$  and BAF1 proteins play roles in proper spindle assembly and positioning, and connect the spindle with the spindle matrix. Previous studies have shown that pulling and pushing forces generated by astral microtubules contribute to the spindle positioning and orientation (Laan et al., 2012). To test the pulling and pushing forces, we firstly compared the spindle pole astral-microtubule number and length in lamin-A/C, LAP2 $\alpha$  and BAF1 triple-knockdown and control cells. As expected, we found that the number and length of the spindle pole astral microtubules were greatly reduced in lamin-A, LAP2 $\alpha$  and BAF1 knockdown cells at prometaphase and metaphase (Fig. 6A,B). More significantly, the astral microtubules in lamin-A/C, LAP2 $\alpha$  and BAF1 knockdown cells could not touch the cell cortex, regardless of whether the spindle was symmetrical, asymmetrical or abnormally localized (Fig. 6A,B; supplementary material Fig. S4). These results are also consistent with those mentioned above – that knocking down these proteins results in short metaphase spindles (Fig. 2E,F).

As the lamin-A/C, LAP2 $\alpha$  and BAF1 proteins co-localize on the spindle and cell cortex, we attempted to determine whether they function independently or synergistically. Cells that stably expressed GFP–lamin-A (Fig. 6C) and GFP–BAF1 (Fig. 6D) were synchronized in prometaphase by using nocodazole. The GFP-tagged proteins were immunoprecipitated using an antibody against GFP, and the proteins that had co-immunoprecipitated with the GFP-tagged proteins were probed with antibodies against LAP2 $\alpha$ , lamin-A/C or BAF1. The results showed that the endogenous LAP2 $\alpha$  and BAF1 proteins co-immunoprecipitated with GFP–lamin-A, and endogenous lamin-A/C and LAP2 $\alpha$  co-immunoprecipitated with GFP–BAF1 (Fig. 6C,D), implying that these proteins were in a complex. We also knocked down the endogenous lamin-A/C in cells that stably expressed GFP–BAF1 by using small interfering (si)RNA. We then arrested the cells at prometaphase by using nocodazole, immunoprecipitated GFP–BAF1 and used western blotting to detect LAP2 $\alpha$ . The result showed that knocking down lamin-A severely affected the binding of LAP2 $\alpha$  to GFP–BAF1 (Fig. 6E). Similarly, when endogenous BAF1 was knocked down in GFP–lamin-A-expressing cells, the binding of LAP2 $\alpha$  to GFP–lamin-A was disrupted (Fig. 6F). From these results, we conclude that lamin-A/C, LAP2 $\alpha$  and BAF1 form a stable protein complex.



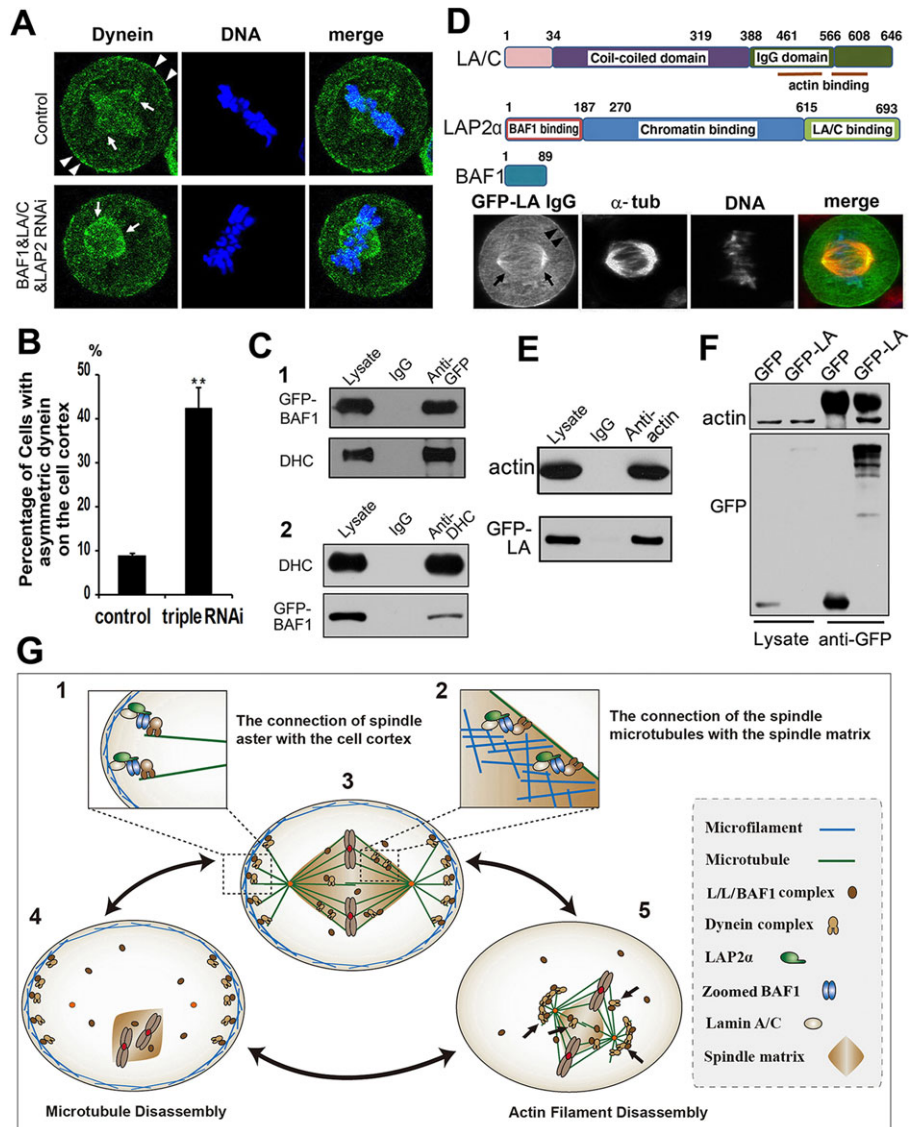


**Fig. 7. The mechanism by which the lamin-A/C–LAP2 $\alpha$ –BAF1 complex regulates the mitotic spindle assembly, positioning and orientation.** (A) Cells with lamin-A/C, LAP2 $\alpha$  and BAF1 triple-knockdown were immunostained for dynein using an antibody specific for the dynein heavy chain. DNA was labeled with DAPI. Note that in the control cell, dynein was concentrated in the spindle (arrows) and the cell cortex area nearest to the spindle poles (arrowheads). However, in the lamin-A/C, LAP2 $\alpha$  and BAF1 triple-knockdown cell (BAF1&LA/C&LAP2 RNAi), the localization of dynein in the cell cortex was uneven, and its localization at the spindle became more condensed and aggregated (arrows). (B) Quantification of the percentages of the metaphase cells with asymmetrical localization of dynein at the cell cortex. Three independent experiments were performed; \*\* $P < 0.01$ . Data are means  $\pm$  s.d. (C) GFP–BAF1 was immunoprecipitated with an antibody against GFP from the lysate of mitotic HeLa cells that stably expressed GFP–BAF1, and the co-immunoprecipitated proteins were probed with an antibody against dynein heavy chain (DHC) (panel 1); the cell lysate was immunoprecipitated with an antibody against DHC and the co-immunoprecipitated proteins were probed with an antibody against GFP to detect GFP–BAF1 (panel 2). Note that both BAF1 and DHC were co-immunoprecipitated, suggesting that BAF1 links the lamin-A/C–LAP2 $\alpha$ –BAF1 complex to dynein. (D) The IgG domain of lamin-A/C (LA/C) binds to actin filaments in the cell cortex and spindle matrix. The upper panel shows a diagram of the relevant domains in lamin-A/C, LAP2 $\alpha$  and BAF1, whereas the lower panel shows the location of the lamin-A/C IgG (GFP–LA IgG) domain when expressed. Note that the IgG domain of lamin-A/C was concentrated in the spindle area (arrows) and the cell cortex (arrowheads).  $\alpha$ -tub,  $\alpha$ -tubulin. (E, F) Lamin-A/C binds to actin filaments in double-thymidine released mitotic cells. GFP–lamin-A was immunoprecipitated, using an antibody against GFP, from the lysate of mitotic HeLa cells, and the co-immunoprecipitated proteins were probed with an antibody against actin. Note that lamin-A/C (GFP–LA) and actin were co-immunoprecipitated. (G) A model to elucidate the mechanism by which the lamin-A/C–LAP2 $\alpha$ –BAF1 complex (L/L/BAF1 complex) regulates the mitotic spindle assembly, positioning and orientation. When the cell enters mitosis, lamin-A/C, LAP2 $\alpha$  and BAF1 disassociate from the interphase nuclear periphery, and relocate to the mitotic spindle and cell cortex where they form a stable protein complex that binds to actin–myosin filaments through the IgG domain of lamin (steps 1 and 2). Simultaneously, the protein complex binds to the motor protein dynein on the spindle and astral microtubules through BAF1, resulting in connection of the astral microtubules with the cell cortex (step 1) and the spindle microtubules with the spindle matrix (step 2). Through a balance of pulling and pushing forces between the spindle and the cell cortex, which is generated by dynein, the spindle is properly positioned and oriented in the cell (step 3). When a microtubule-disassembly-inducing drug is used to disrupt the spindle and astral microtubules, the connection of the spindle with the cell cortex and spindle matrix is disrupted (step 4). Accordingly, the chromosomes and the spindle matrix lose their original position and randomly localize in an area of the cytoplasm, whereas the lamin-A/C–LAP2 $\alpha$ –BAF1 complex and dynein concentrate in the cell cortex (step 4). When a drug is used to specifically disassemble actin–myosin-II filaments, the connection of the spindle with the cell cortex and spindle matrix is disrupted, leading to withdrawal from the cell cortex of the aster microtubules with the lamin-A/C–LAP2 $\alpha$ –BAF1 complex and to the formation of a swollen short spindle and the shrinkage of the spindle matrix, which associates with lamin-A/C–LAP2 $\alpha$ –BAF1 complexes and dynein proteins (step 5, arrows).

To understand how knocking down the lamin-A/C, LAP2 $\alpha$  and BAF1 protein complex results in disconnection of the mitotic spindle from the cell cortex and spindle matrix, we immunostained the cells with an antibody specific for dynein (recognizing dynein heavy chain, DHC), one of the pulling-force generators (Kozlowski et al., 2007; Laan et al., 2012). We observed that a fraction of dynein was concentrated in the spindle and the cell cortex areas opposite to the spindle poles in the control cells, whereas the cell cortex location of dynein proteins was changed in lamin-A, LAP2 $\alpha$  and BAF1 triple-knockdown cells (Fig. 7A,B). Therefore, we performed a co-immunoprecipitation assay by using a diluted lysate of mitotic cells that stably expressed GFP–BAF1, and found that BAF1 and dynein could be co-immunoprecipitated (Fig. 7C). We also investigated how the protein complex links the astral microtubules to the cell cortex, and the spindle microtubules to the spindle matrix. Because it is known that lamin-A/C has an IgG domain that can directly interact with actin filaments and that LAP2 $\alpha$  directly binds to lamin-A/C and BAF1 (Dechat et al., 2000; Simon et al., 2010), we first expressed the lamin-A/C IgG domain (from amino acid residues 425 to 525), which had been tagged with GFP, in cells to determine the localization of this IgG domain. The results clearly showed that the IgG domain localized in the cell cortex and the spindle area (Fig. 7D), and that lamin-A/C and actin could be co-immunoprecipitated in mitotic cells (Fig. 7E,F). Because previous studies have shown that the lamin-A/C IgG domain can bind to actin *in vitro*, this lamin-A/C–LAP2 $\alpha$ –BAF1 protein complex probably binds to actin filaments in the cell cortex and in the spindle matrix through the IgG domain of lamin-A/C proteins. Taken together, these results indicate that the lamin-A/C–LAP2 $\alpha$ –BAF1 protein complex binds to actin filaments of the cell cortex through lamin-A/C, and to microtubules of the aster and spindle through interaction of BAF1 with microtubule-associated dynein proteins.

## DISCUSSION

The disassembly and reassembly of the nucleus is dynamic during the cell cycle. Along with disassembly of the nucleus during mitotic entry, the nuclear envelope becomes fragmented and disperses into the cytoplasm, whereas its chromatin condenses into chromosomes. The mitotic spindle is another dynamic organelle during the cell cycle. It also assembles at mitotic entry and connects with the kinetochores of the chromosomes. It is known that some proteins shuttle between the nucleus and the spindle during the cell cycle in order to perform distinct functions, although few of these proteins and functions are recognized. NuMA is an example of such a protein, which is localized at the interphase nucleus and might function to maintain the nuclear structures (Harborth et al., 1999); however, in mitosis, it relocates to the spindle and serves as one of the SAFs to regulate spindle assembly (Clarke and Zhang, 2008; Wiese et al., 2001). Another example is the lamin-B protein, which contributes to the assembly of the nuclear periphery, to the maintenance and function of the nuclear lamina in interphase, and to the structure and function of the spindle matrix in mitosis (Tsai et al., 2006). Therefore, the shuttling of proteins from the interphase cell nucleus to the mitotic cell organelles in order to perform distinct functions is essential; the shuttling of proteins is also a common event in the varying phases of the cell cycle. However, many of these proteins, and their distinct functions at different organelles at different stages of the cell cycle are, so far, largely unknown.

Here, we found that the nuclear periphery proteins lamin-A/C, LAP2 $\alpha$  and BAF1, which play crucial roles in maintaining the interphase nuclear structure and function (Gruenbaum et al., 2005;

Hutchison, 2002; Simon and Wilson, 2011), are relocated to the mitotic spindle and the cell cortex in mitosis to regulate mitotic spindle assembly and positioning. However, how these proteins perform their mitotic function is, so far, not very clear, although it is known that they are assembled into a protein complex. Nevertheless, owing to the fact that LAP2 $\alpha$  can directly bind to lamin-A/C and BAF1 through its C-terminus and LEM domain, we propose that they directly form a protein complex in order to perform their functions during mitosis; however, we do not exclude the possibility that other factors could have a role. Furthermore, because lamin-A/C has an IgG domain that might bind to actin, we believe that this protein complex binds to the actin filaments in the cell cortex and the spindle matrix through lamin-A/C. Moreover, because BAF1 can directly bind to the microtubule-associated protein dynein, we propose that BAF1 targets the protein complex to the microtubules through interaction with dynein. Consequently, in mitosis, this protein complex might target itself to the microtubules of the mitotic spindle and/or pole asters through the interaction of BAF1 at one site with the microtubule-associated dynein, and then link the spindle to the cell cortex and spindle matrix through interaction of lamin-A/C at another site with the actin filaments on both the cell cortex and the spindle matrix.

Based on these results, we propose a unique model in order to illustrate the mechanism of how the lamin-A/C–LAP2 $\alpha$ –BAF1 complex functions to regulate mitotic spindle assembly and positioning in mitosis (Fig. 7G). During the G2/M phase transition, lamin-A/C, LAP2 $\alpha$  and BAF1 disassociate from the interphase nuclear periphery and assemble into a stable complex. This protein complex binds to the actin–myosin filaments in the cell cortex to anchor itself to it. Simultaneously, the protein complex binds to dynein on the microtubules of the spindle and pole asters, resulting in the connection of the aster microtubules to the cell cortex. Through a balance of pulling and pushing forces between the spindle and the cell cortex, which are generated by dynein, the spindle is properly positioned and orientated. Collectively, this work might have important implications in understanding how the nuclear periphery proteins perform distinct functions in interphase and mitosis.

## MATERIALS AND METHODS

### Antibodies

Two antibodies against BAF1 (sc-166324 and sc-33787) were obtained from Santa Cruz Biotechnology (Santa Cruz, CA), and two monoclonal antibodies against  $\gamma$ -tubulin and  $\alpha$ -tubulin (T3559 and T9026) were obtained from Sigma-Aldrich. Antibodies against lamin-B1 (ab16048), NuMA (ab10530), LAP2 $\alpha$  (ab66588), dynein heavy chain (ab6305) and lamin-A/C (ab8980) were obtained from Abcam (Cambridge, UK). Secondary antibodies used were Alexa-Fluor-488 donkey anti-mouse IgG, Alexa-Fluor-546 donkey anti-mouse IgG, Alexa-Fluor-546 donkey anti-rabbit and horse radish peroxidase (HRP)-conjugated goat anti-rabbit or anti-mouse IgG were obtained from Invitrogen. Two additional antibodies against lamin-A/C and GFP were generated in-house by immunizing rabbits with GST-tagged lamin-A/C peptide (amino acid residues 425–525) and His-tagged GFP. All animal experiments were performed according to approved guidelines.

### Cell culture and siRNA transfection

HeLa cells were maintained in Dulbecco's modified Eagle's medium supplemented with 10% bovine calf serum, 100 U/ml penicillin and 100  $\mu$ g/ml streptomycin (all from Hyclone) at 37°C and 5% CO<sub>2</sub>. Subclones of HeLa cell lines that stably expressed GFP– $\alpha$ -tubulin, GFP–BAF1 and GFP–lamin-A were generated by selecting with G418. To synchronize cells into mitosis for immunoprecipitation assays or immunofluorescence labeling, HeLa cells were treated with thymidine, released for 10 h, and then supplemented with 100 nM/ml nocodazole for another 6 h. RNAi

experiments were performed by using siRNAs against BAF1 (number 1 5'-CAGUCACUGUCCUUGUAAATT-3', number 2 5'-GCCAGUUUCUG-GUGCUAAATT-3' and number 3 5'-GGCUGGGAUUGGUGAAGUC-TT-3'), lamin-A/C (number 1 5'-GCUCGCAACAAGUCCAAUTT-3', number 2 5'-CCCUUGACUCAGUAGCCAATT-3' and number 3 5'-CACCAAAGUUCACCCUGAATT-3'), LAP2 $\alpha$  (number 1 5'-GCAG-AAUGGAAGUAAUGAUTT-3', number 2 5'-GCAGAUGUCAAGU-CAGAAATT-3' and number 3 5'-CAGGAAGCUAUUGAGAAATT-3'). For RNAi rescue experiments, the genes encoding lamin-A/C, LAP2 $\alpha$  and BAF1 were cloned and inserted into the RNAi-resistant GFP-C2 vector. The primers used to generate the RNAi-resistant vector were as follows: BAF1, number 1 5'-CAATCGCGAGATTGATTTGGT-3', number 2 5'-GGACAATTCTAGTTCACAAG-3' and number 3 5'-CTAGCCGGAATCGGCGAGGTT-3'; lamin-A/C, number 1 5'-CT-ACGAAATAAATTAACGAAGAT-3', number 2 5'-AAAACCTCTCG-ATTCCGTCGCA-3' and number 3 5'-CCTCCGAAGTTTACGCTAA-AG-3'; LAP2 $\alpha$ , number 1 5'-CAAAACGGTAGCAACGACTCA-3', number 2 5'-AGGGAATAAGTGAACCTACTA-3' and number 3 5'-AG-AAAACCTACTCGAAAAGAAG-3'.

### Immunofluorescence microscopy

Cells were grown on coverslips and fixed in 4% paraformaldehyde or 10% trichloroacetic acid at room temperature for 15 min. The cells were permeabilized with 0.1% Triton X-100 for 5 min and incubated with primary antibodies for 1 h at room temperature. After washing in PBS, the cells were incubated with secondary antibodies for 1 h at room temperature. Coverslips were mounted with Mowiol with 1 mg/ml DAPI for DNA staining, and analyzed with standard FITC and TRITC, Rhodamine and DAPI filter sets on a ZEISS 200 M immunofluorescence microscope. Images were captured with cool CCD and Axiovert image software.

### Live-cell imaging and microscopy

HeLa cells that stably expressed GFP- $\alpha$ -tubulin or transiently expressed the indicated GFP-, YFP- or mCherry-tagged proteins were plated in glass-bottomed dishes and directly processed for live imaging. Data were acquired by using a DeltaVision live-cell imaging system (Applied Precision) equipped with an Olympus IX-71 inverted microscope and a 60 $\times$ /1.42 oil objective. Images of the fixed cells were captured by using a CoolSnap HQ2 CCD camera equipped with a Zeiss LSM710 confocal microscope, and different z-sections were deconvolved by using the SoftWorx suite and maximum intensity projections.

### Microtubule regrowth assay

Mitotic cells that had been transfected with control siRNAs, or siRNAs against lamin-A/C, LAP2 $\alpha$  or BAF1 were treated on ice for 40 min to completely depolymerize the microtubules; then the cells were released into warm medium to allow microtubule regrowth for the times indicated. Then, the cells were fixed and immunostained with an antibody against  $\alpha$ -tubulin.

### Immunoprecipitation

HeLa cells were lysed in RIPA buffer or lysis buffer, comprising 1% NP-40, 20 mM Tris-HCl (pH 7.4), 150 mM NaCl, 0.5 mM EGTA, 10 mM NaF and 1 mM PMSF. Mitotic cells were isolated by using treatment with Nocodazole and then shaking the cells off of the cell culture; mitosis was confirmed by DNA staining and western blotting of phosphorylated histone H3 at residue Ser10 (supplementary material Fig. S4E–G). For immunoprecipitation, mitotic HeLa cells that transiently expressed GFP-BAF1 or GFP-lamin-A were harvested by shaking them off; cells were then lysed at 4°C for 30 min and centrifuged. The supernatant of the cell lysate was incubated with protein-A beads coupled with an antibody against GFP for 4 h at 4°C. The beads were collected by centrifugation and washed with RIPA buffer. The immunoprecipitated proteins were separated by using SDS-PAGE gels and were then immunoblotted with the indicated antibodies.

### Acknowledgements

We thank the other members of our laboratory for critical discussion and helpful comments on this work. We thank Dr Jianguo Chen (College of Life Sciences, Peking University, Beijing, China) for providing the GFP-EB3 vector.

### Competing interests

The authors declare no competing or financial interests.

### Author contributions

R.Q., N.X., G.W., H.R., S.L., J.L., Q.L., L.W. and X.G. conceived and performed the experiments; C.Z., Q. J., H.Z., R.Q. and N.X. analyzed and interpreted the data; C.Z., Q.J., R.Q. and N.X. wrote the paper.

### Funding

This work was supported by grants from the National Natural Science Foundation of China (NSFC) [grant numbers 91313302, 31030044 and 31371365]; and the State Key Basic Research and Development Plan of Ministry of Science and Technology of China [grant numbers 2010CB833705 and 2014CB138402].

### Supplementary material

Supplementary material available online at <http://jcs.biologists.org/lookup/suppl/doi:10.1242/jcs.164566/-/DC1>

### References

- Azoury, J., Lee, K. W., Georget, V., Rassiniere, P., Leader, B. and Verlhac, M.-H. (2008). Spindle positioning in mouse oocytes relies on a dynamic meshwork of actin filaments. *Curr. Biol.* **18**, 1514–1519.
- Burke, B. and Stewart, C. L. (2002). Life at the edge: the nuclear envelope and human disease. *Nat. Rev. Mol. Cell Biol.* **3**, 575–585.
- Burke, B. and Stewart, C. L. (2006). The laminopathies: the functional architecture of the nucleus and its contribution to disease. *Annu. Rev. Genome Hum. Gen.* **7**, 369–405.
- Burke, B. and Stewart, C. (2013). The nuclear lamins: flexibility in function. *Nat. Rev. Mol. Cell Biol.* **14**, 13–24.
- Clarke, P. R. and Zhang, C. (2008). Spatial and temporal coordination of mitosis by Ran GTPase. *Nat. Rev. Mol. Cell Biol.* **9**, 464–477.
- Dechat, T., Korbei, B., Vaughan, O. A., Visek, S., Hutchison, C. J. and Foisner, R. (2000). Lamina-associated polypeptide 2 $\alpha$  binds intranuclear A-type lamins. *J. Cell Sci.* **113**, 3473–3484.
- Fu, W., Tao, W., Zheng, P., Fu, J., Bian, M., Jiang, Q., Clarke, P. R. and Zhang, C. (2010). Clathrin recruits phosphorylated TACC3 to spindle poles for bipolar spindle assembly and chromosome alignment. *J. Cell Sci.* **123**, 3645–3651.
- Galli, M., Muñoz, J., Portegijs, V., Boxem, M., Grill, S. W., Heck, A. J. R. and van den Heuvel, S. (2011). aPKC phosphorylates NuMA-related LIN-5 to position the mitotic spindle during asymmetric division. *Nat. Cell Biol.* **13**, 1132–1138.
- Gesson, K., Vidak, S. and Foisner, R. (2014). Lamina-associated polypeptide (LAP)2 $\alpha$  and nucleoplasmic lamins in adult stem cell regulation and disease. *Semin. Cell Dev. Biol.* **29**, 116–124.
- Grill, S. W. and Hyman, A. A. (2005). Spindle positioning by cortical pulling forces. *Dev. Cell* **8**, 461–465.
- Gruenbaum, Y., Margalit, A., Goldman, R. D., Shumaker, D. K. and Wilson, K. L. (2005). The nuclear lamina comes of age. *Nat. Rev. Mol. Cell Biol.* **6**, 21–31.
- Güttinger, S., Laurell, E. and Kutay, U. (2009). Orchestrating nuclear envelope disassembly and reassembly during mitosis. *Nat. Rev. Mol. Cell Biol.* **10**, 178–191.
- Harborth, J., Wang, J., Gueth-Hallonet, C., Weber, K. and Osborn, M. (1999). Self assembly of NuMA: multiarm oligomers as structural units of a nuclear lattice. *EMBO J.* **18**, 1689–1700.
- Hutchison, C. J. (2002). Lamins: building blocks or regulators of gene expression? *Nat. Rev. Mol. Cell Biol.* **3**, 848–858.
- Kiyomitsu, T. and Cheeseman, I. M. (2012). Chromosome- and spindle-pole-derived signals generate an intrinsic code for spindle position and orientation. *Nat. Cell Biol.* **14**, 311–317.
- Kozlowski, C., Srayko, M. and Nedelec, F. (2007). Cortical microtubule contacts position the spindle in *C. elegans* embryos. *Cell* **129**, 499–510.
- Laan, L., Pavin, N., Husson, J., Romet-Lemonne, G., van Duijn, M., López, M. P., Vale, R. D., Jülicher, F., Reck-Peterson, S. L. and Dogterom, M. (2012). Cortical dynein controls microtubule dynamics to generate pulling forces that position microtubule asters. *Cell* **148**, 502–514.
- Lancaster, O. M. and Baum, B. (2011). Might makes right: using force to align the mitotic spindle. *Nat. Cell Biol.* **13**, 736–738.
- Luxenburg, C., Amalia Pasolli, H., Williams, S. E. and Fuchs, E. (2011). Developmental roles for Srf, cortical cytoskeleton and cell shape in epidermal spindle orientation. *Nat. Cell Biol.* **13**, 203–214.
- Margalit, A., Segura-Totten, M., Gruenbaum, Y. and Wilson, K. L. (2005). Barrier-to-autointegration factor is required to segregate and enclose chromosomes within the nuclear envelope and assemble the nuclear lamina. *Proc. Natl. Acad. Sci. USA* **102**, 3290–3295.
- Markus, S. M. and Lee, W.-L. (2011). Microtubule-dependent path to the cell cortex for cytoplasmic dynein in mitotic spindle orientation. *Bioarchitecture* **1**, 209–215.
- Mekhail, K. and Moazed, D. (2010). The nuclear envelope in genome organization, expression and stability. *Nat. Rev. Mol. Cell Biol.* **11**, 317–328.
- Orjalo, A. V., Arnaoutov, A., Shen, Z., Boyarchuk, Y., Zeitlin, S. G., Fontoura, B., Briggs, S., Dasso, M. and Forbes, D. J. (2006). The Nup107-160 nucleoporin

- complex is required for correct bipolar spindle assembly. *Mol. Biol. Cell* **17**, 3806-3818.
- Pekovic, V., Harborth, J., Broers, J. L. V., Ramaekers, F. C. S., van Engelen, B., Lammens, M., von Zglinicki, T., Foisner, R., Hutchison, C. and Markiewicz, E.** (2007). Nucleoplasmic LAP2 $\alpha$ -lamin A complexes are required to maintain a proliferative state in human fibroblasts. *J. Cell Biol.* **176**, 163-172.
- Puente, X., Quesada, V., Osorio, F. G., Cabanillas, R., Cadiñanos, J., Fraile, J. M., Ordóñez, G., Puente, D. A., Gutiérrez-Fernández, A., Fanjul-Fernández, M. et al.** (2011). Exome sequencing and functional analysis identifies BANF1 mutation as the cause of a hereditary progeroid syndrome. *Am. J. Hum. Gen.* **88**, 650-656.
- Rosenblatt, J., Cramer, L. P., Baum, B. and McGee, K. M.** (2004). Myosin II-dependent cortical movement is required for centrosome separation and positioning during mitotic spindle assembly. *Cell* **117**, 361-372.
- Scholey, J. M., Brust-Mascher, I. and Mogilner, A.** (2003). Cell division. *Nature* **422**, 746-752.
- Simon, D. N. and Wilson, K. L.** (2011). The nucleoskeleton as a genome-associated dynamic 'network of networks'. *Nat. Rev. Mol. Cell Biol.* **12**, 695-708.
- Simon, D., Zastrow, M. S. and Wilson, K. L.** (2010). Direct actin binding to A- and B-type lamin tails and actin filament bundling by the lamin A tail. *Nucleus* **1**, 264-272.
- Tsai, M.-Y., Wang, S., Heidinger, J. M., Shumaker, D. K., Adam, S. A., Goldman, R. D. and Zheng, Y.** (2006). A mitotic lamin B matrix induced by RanGTP required for spindle assembly. *Science* **311**, 1887-1893.
- Verhac, M.-H.** (2011). Spindle positioning: going against the actin flow. *Nat. Cell Biol.* **13**, 1183-1185.
- Verstraeten, V. L. R. M., Broers, J. L. V., Ramaekers, F. C. S. and van Steensel, M. A. M.** (2007). The nuclear envelope, a key structure in cellular integrity and gene expression. *Curr. Med. Chem.* **14**, 1231-1248.
- Walczak, C. E. and Heald, R.** (2008). Mechanisms of mitotic spindle assembly and function. *Int. Rev. Cytol.* **265**, 111-158.
- Weber, K. L., Sokac, A. M., Berg, J. S., Cheney, R. E. and Bement, W. M.** (2004). A microtubule-binding myosin required for nuclear anchoring and spindle assembly. *Nature* **431**, 325-329.
- Wiese, C., Wilde, A., Moore, M. S., Adam, S. A., Merdes, A. and Zheng, Y.** (2001). Role of importin-beta in coupling Ran to downstream targets in microtubule assembly. *Science* **291**, 653-656.
- Wühr, M., Mitchison, T. J. and Field, C. M.** (2008). Mitosis: new roles for myosin-X and actin at the spindle. *Curr. Biol.* **18**, R912-R914.
- Yao, C., Rath, U., Maiato, H., Sharp, D., Girton, J., Johansen, K. M. and Johansen, J.** (2012). A nuclear-derived proteinaceous matrix embeds the microtubule spindle apparatus during mitosis. *Mol. Biol. Cell* **23**, 3252-3541.
- Yi, K., Unruh, J. R., Deng, M., Slaughter, B. D., Rubinstein, B. and Li, R.** (2011). Dynamic maintenance of asymmetric meiotic spindle position through Arp2/3-complex-driven cytoplasmic streaming in mouse oocytes. *Nat. Cell Biol.* **13**, 1252-1258.
- Zheng, Y.** (2010). A membranous spindle matrix orchestrates cell division. *Nat. Rev. Mol. Cell Biol.* **11**, 529-535.
- Zheng, R., Ghirlando, R., Lee, M. S., Mizuuchi, K., Krause, M. and Craigie, R.** (2000). Barrier-to-autointegration factor (BAF) bridges DNA in a discrete, higher-order nucleoprotein complex. *Proc. Natl. Acad. Sci. USA* **97**, 8997-9002.